Drawing Velocity Regulation for Thermoplastic Micro-forming of Bulk Metallic Glass Drawing Process

WCMNM 2021

Nattasit Dancholvichit, Srinivasa Salapaka, Shiv Kapoor

Department of Mechanical Science and Engineering, University of Illinois: Urbana-Champaign, Urbana, IL 61801

Abstract

Drawing velocity is essential to the manufacturing of the multi-facet bulk metallic glass (BMG) surgical-grade knife blade cutting edges since it is one of the factors that can determine good blade edge profiles in the thermoplastic forming process. The goal of this paper is to determine and regulate drawing velocity based on the viscoelastic filament stretching process and knowledge of the thermoplastic forming map of BMG. The generation of drawing velocity profile is done in two stages: the initial transient stage before the extensional viscosity stage is fully developed, and the extensional viscosity stage. The controller based on the system identification of the testbed is then optimized from the requirements of the drawing velocity and its implementation feasibility. The control objectives of regulation performance and robustness to modeling uncertainties are posed and solved in an optimal control (H_∞) framework. The proposed controller shows an improvement over other controllers including PID controllers in terms of robustness to uncertainties and tracking performance. BMG samples processed from this study result in good quality with better straightness and more consistent blade edge radii.

Keywords: Micro-manufacturing; Robust Control; Process Modelling; Metallic Glass

1. Introduction

Bulk metallic glass (BMG) due to its high strength, hardness, and biocompatibility at room temperature is a good alternative material for manufacturing surgical blades [1]. When supercooled, BMG exhibits superplastic flow as a function of temperature and strain rate [2]. Further, during the Newtonian flow the stress-induced free volume is quickly redistributed via rearrangements of local atoms thereby allowing perfectly plastic behavior [2]. This property motivated us to develop a testbed that can manufacture surgical-grade knife blade cutting edges from Vitreloy-1b (Vit-1b). In this setup, we have enabled thermally-assisted micro molding and thermally-assisted micro drawing process [3–5]. Apart from maintaining the temperature of the BMG sample, the drawing velocity is found to be a significant parameter that determines the shape of the resulting blade edges. Poorly controlled drawing velocities lead to inappropriate strain rates, which cause abrupt shifts to viscosity deformations. This undesired transition between Newtonian and Non-Newtonian regimes can lead to shear-localized failure [2], and hence result in blade edges with poor finish [3,4].

In previous studies, voice call actuators (VCAs) use proportional-integral-derivative (PID) controllers [3–5] to track reference signal $V_{ref}(t)$. However, the existing control strategies are unable to produce blade edges consistently with desired shape specifications. The main reasons for this inconsistency are inadequately designed $V_{ref}(t)$, which do not guarantee forays into non-Newtonian regimes, and limited control designs that do not address large uncertainties in the drawing processes. It therefore is critical to come up with a new velocity profile $V_{ref}(t)$, which when tracked will enable consistency in manufacturing good quality blade edges. Besides, the drawing velocity controllers must be capable of accurately tracking the reference trajectories, while being robust to disturbances and other modeling uncertainties, and thus improving the repeatability of the process.

In this article, we address these challenges – we design $V_{ref}(t)$ such that the ensuing strain rates guarantee homogeneous deformations of the BMG sample. $V_{ref}(t)$ is generated using the viscoelastic filament stretching model that describes the drawing process of BMG and using the experimental data that result in good quality blade edges. Based on system identification of the drawing module, an H_∞ control architecture is proposed and implemented on the thermoplastic forming testbed. The main challenges in control design are achieving the temporal bandwidths imposed by the velocity profile $V_{ref}(t)$ and guaranteeing robustness to uncertainties inherent in the drawing process. The performance of the implemented controller is presented and compared to the PID counterpart. Further, the experimental results of the manufactured blades based on the proposed controller are provided.

2. Drawing velocity profile

We first introduce the thermoplastic drawing process, and use it to develop the velocity profile, $V_{ref}(t)$ as well as its transitional mechanism. Then, we analyze $V_{ref}(t)$ to assess the range of its frequency components, and specify the tracking bandwidth requirements on the controller design.

2.1 Thermoplastic drawing process

The thermoplastic drawing process of the BMG sample is illustrated in Fig. 1 (a) [3]. After the sample is heated and molded at the desired temperature T_d and initial mold gap D_o, the sample is clamped and drawn at velocity, $V(t)$ from the initial distance, L_o. The thermoplastic drawing process forms the blade edge with diameter $D_{mid}(t)$ for a drawing distance of $L(t)$.

Here, thermoplastic forming of the BMG sample is viewed as a viscoelastic stretching process of a filament, where viscoelastic, capillary, inertial, and oxidation effects are included. Many theoretical, simulation, and experimental studies of the filament stretching process have been published that can accurately predict the breakup profile of the viscoelastic fluid filaments. More recently, Anna et. al [6,7] reported that using the constitutive model

developed from mass conservation and force balance equations, filament diameter profile based on the drawing position can be predicted. The assumptions of this one-dimensional constitutive model include symmetric slender filament approximation at midplane, $\Lambda(t) = \frac{2L(t)}{D_{mid}(t)} \gg 1$, and small Reynolds number, $Re = \rho V L/\eta \ll 1$, where ρ and η are the density and the viscosity of the material. Note that these assumptions of the filament breakup model are also applicable to the BMG drawing process. Besides, the oxidation layer effects of BMG are insignificant since the operating temperature is well below crystallization temperature. In their study of the evolution of breakup profile, Anna et al. found that when a filament is drawn with a constant elongation rate, $\dot{E}_{II}$, for a distance, $L(t) = L_o exp(\dot{E}_{II} t)$, the filament diameter $D_{mid}(t)$ can be expressed as [7];

$$D_{mid}(t) = A_D \exp(-tB_D) + C_D t + D_D, \qquad (1)$$

where A_D, B_D, C_D and D_D are parameters, which can be determined from the sample geometry, initial conditions of the draw, and material properties [7,8].

To compare the blade edge profile evolution of BMG drawing to the filament breakup model, the BMG samples are drawn at constant $\dot{E}_{II}$. $D_{mid}(t)$ of the drawn BMG blade edge profile measured by Keyence confocal microscope is shown in Fig. 1 (b) along with its regression fit of the filament sample diameter given in Eq (1). As seen in Fig. 1 (b), $D_{mid}(t)$ of BMG sample matches well with the predicted profile suggesting that the behavior of thermoplastic drawing of BMG agrees with the filament stretching model; except at the initial stage. This suggests that the BMG thermoplastic forming process can be viewed as a viscoelastic stretching process only after the extensional viscosity is fully developed. Similar behavior of transient behavior has also been observed in liquid stretching in the trapezoidal cavity due to different mold geometry and initial contact angle [9]. At a finite time, as $D_{mid}(t)$ decreases sharply (roughly after 20 seconds), the filament breaks due to the capillary instability.

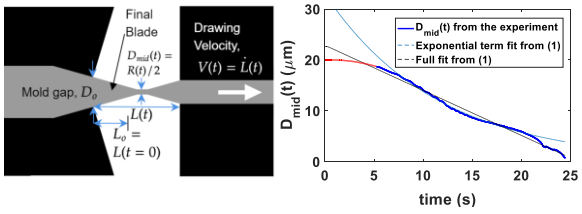

(a) (b)

Fig. 1. (a) Schematic of BMG drawing process; **(b)** Diameter of the blade profile

2.2 Reference Velocity Generation

To accommodate the transient behavior of the drawing process, $V_{ref}(t)$ is designed to comprise of two stages: the initial transient stage, $V_{ref,t}(t)$, before the extensional viscosity stage is fully developed, and the extensional viscosity stage, $V_{ref,v}(t)$.

The velocity during the extensional viscosity is obtained by $V_{ref,v}(t) = \frac{d}{dt}\left(L_{ref,v}(t)\right)$, where the position reference $L_{ref,v}(t)$ is derived from a model for drawing distance in the viscoelastic stretching process, which is given as [7,8]

$$L_{ref,v}(t) = L_o \exp\left\{\int (\dot{\varepsilon}_{eff}(t)/\dot{E}(t))^{-1} \dot{\varepsilon}_o dt\right\}, \qquad (2)$$

where $\dot{\varepsilon}_{eff}(t)/\dot{E}(t)$ represents the constitutive response from viscosity resulting from temperature, geometry, and deformation history of BMG from a Newtonian blade edge profile. $L_{ref,v}(t)$ is computed using Eq (2), where the effective deformation rate $\dot{\varepsilon}_{eff}$ and the extensional rate $\dot{E}(t)$ are given by;

$$\dot{\varepsilon}_{eff} = (-2/D_{mid}(t))(\mathrm{d}D_{\mathrm{mid}}(\mathrm{t})/dt), \qquad (3)$$

$$\dot{E}(t) = \dot{L}(t)/L(t). \qquad (4)$$

Here $D_{mid}(t)$, the drawing distance $L(t)$, and velocity term $\dot{L}(t)$ can be obtained from blade edge profile data from the drawing experiments in the Newtonian region. To obtain $L_{ref,v}(t)$, $\dot{\varepsilon}_o$ is chosen from the thermoplastic forming map that yields good blade [2].

The velocity profile of the initial transient stage $V_{ref,t}(t)$ of the drawing process is chosen to be constant in order to guarantee the homogeneous flow of BMG within the deformation map [2]. From several drawing experiments, we deduced that $V_{ref,t}(t)$ of 0.01 mm/s is sufficient to successfully transition BMG sample from stationary to the transient stage without triggering shear band. A transient stage is to maintain internal structural relaxation of the material to keep up with the external imposed strain rate before the breakup of the material occurs [2]. Note that further studies are needed to accurately obtain $V_{ref,t}(t)$.

To identify the stage at which the transition from $V_{ref,t}(t)$ to $V_{ref,v}(t)$ occurs, we propose to use the change in the drawing force over the distance dF_d/dL_p. At the transient stage, dF_d/dL_p increases until it reaches $\max(dF_d/dL_p)$ and starts decaying. This suggests that the extensional flow is fully developed at $\max(dF_d/dL_p)$ and then gradually transition to extensional flow. This criterion is used to be a transitional point between two stages. For example, in this study, a transition between two stages takes place when $dF_d/dL_p < 0.65\max(dF_d/dL_p)$.

In order to successfully track and control $V_{ref}(t)$, the bandwidth of $V_{ref,v}(t)$ is assessed only as it carries dominant frequencies of $V_{ref}(t)$. Power spectral density of $V_{ref,v}(t)$ is analyzed. The notable peak of the profile indicates the dominant energy of the profile at 0.01 Hz. Hence, the controller must be able to maintain the accuracy of this given bandwidth.

3. Overview of the controller architecture and controller design

A feedback-based control system is developed to make drawing velocity $V(t)$ track $V_{ref}(t)$ accurately within operating bandwidths; thus facilitating consistent good quality necking of the blade edge formation. The hybrid thermoplastic forming testbed is explained in [3,4,10] and shown in Fig. 2 (a). The system consists of VCAs, which provide the necessary force to move the drawing module, and pneumatic, linear encoders, and force sensors that provide measurements for feedback, and a control algorithm implemented on a digital signal processor (LABVIEW). The control algorithm is also designed to make the closed-loop system insensitive (robust) to unmodeled uncertainties such as friction, floor disturbances, and

dynamics of the clamp during the drawing process.

3.1 Overview of the controller architecture

Fig. 2 (b) summarizes the feedback control system architecture and problem formulation block diagram. Here, the transfer function, G, represents the nominal dynamics of the VCA system, and signals d and n respectively represent the disturbances (uncertainties not modeled by G) and the sensor noise. A model for G is obtained by system identification experiments; here a series of sinusoidal inputs $u(t) = 0.018 + 0.01sin(2\pi ft)$, where f varied from 0.01 to 10 Hz, is given to the VCA system. The model is then found by fitting a transfer function to the frequency response obtained from the resulting outputs $V(t)$. The frequency response of the drawing module is shown as G in Fig. 2 (c) where the accuracy of the model is found to be 89%.

The main objective of the controller K is to minimize the tracking error, $e = V_{ref} - V$ over a bandwidth of about 0.12 Hz. Another aspect of the control design is to detect in real-time the fully-developed flow condition during the drawing process and track the corresponding appropriate V_{ref} profile. This detection is done by using the dF_d/dL_p measurements as described in section 2.2 to switch between $V_{ref,t}(t)$ and $V_{ref,v}(t)$.

3.2 H∞ Controller design and implementation

The control design has multiple objectives of accurately tracking within a specified bandwidth, ensuring that the closed-loop system is robust to modeling uncertainties (disturbances and sensor noise) and that control values are within saturation limits. Tuning parameters in traditional methods (such as PID control designs) [11,12] becomes tedious and practically infeasible in view of the multiple objectives. H_∞ control design is used, where an optimization problem that reflects the multiple objectives is solved.

Specifically, in H_∞ control design, the control objective is that the closed-loop tracking error e is made small within a frequency bandwidth and needs to be guaranteed even in the presence of unmanipulable (or prespecified) inputs $V_{ref}(t)$, floor disturbances, and sensor noise. In this design, $z = [W_1 e, W_2 u, W_3 y]$ comprising of weighed tracking error, control signal, output velocity signal, all of which should be small is considered. The H_∞ control design determines a control transfer function K that solves the optimization problem $\min_{k\in\mathcal{K}} \left\| T_{V_{ref},z} \right\|$ [13], where $T_{V_{ref,}z} = [W_1 S, W_2 KS, W_3 T]$ is the closed-loop transfer function from $V_{ref} \rightarrow [z_1\ z_2\ z_3]$; $S = \frac{1}{1+GK}$, $T = 1 - S$. $\mathcal{K}$ and $\|(\cdot)\|$, respectively and represent the set of all stabilizing controllers and system ∞ norm. For this problem,$|W_1(j\omega)|$ is designed to be high for ω within the tracking bandwidth, and $|W_2(j\omega)|$ and $|W_3(\mathrm{j}\omega)|$ are designed to be high beyond tracking bandwidth to reflect the small tracking error, control effort, and noise attenuation at high frequencies. Note that in addition to low tracking error and control effort, designing for small S also yields robustness (insensitivity) to modeling uncertainties within the tracking bandwidth. The control transfer function is discretized as a biquad filter with a sampling rate of 2000 Hz to ensure stability, reduce quantization effects of the computation, and enable parallel computation in the processor.

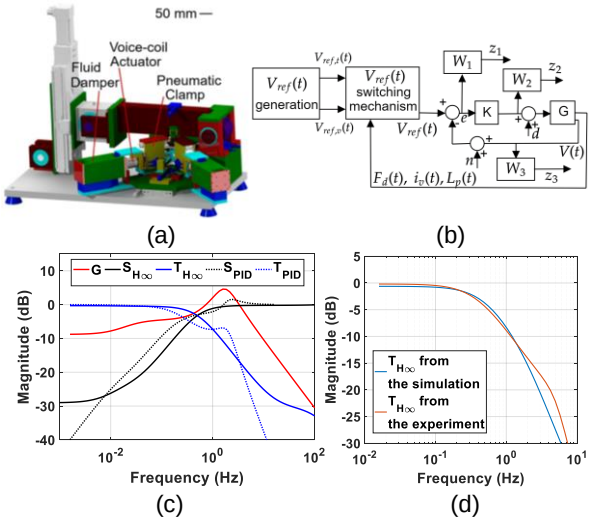

Fig 2. (a) The hybrid thermoplastic forming test bed; **(b)** Block diagram schematic of the proposed controller framework; **(c)** Identified plant (G), sensitivity (S) and complementary sensitivity transfer functions (T) of H_∞ and PID controller (S); **(d)** $T_{H\infty}$ of simulation vs experiment.

4. Results and discussion

The closed-loop sensitivity transfer function S (from $V_{ref} \rightarrow e$) and complementary sensitivity transfer function T (from $V_{ref} \rightarrow V$) of the proposed controller and a PID design (after much tuning) are shown in Fig. 2 (c). At low frequency, the proposed controller is robust against disturbances as seen in low $\|S_{H_\infty}\|$ value with a -3dB cutoff frequency of 0.45 Hz, which is better than the previously implemented PID controller. $\|S_{H_\infty}\|$ is lower than $\|S_{PID}\|$ throughout the frequency of interest at 0.01 Hz to 0.5 Hz, which implies better robustness to unmodeled dynamics [13]. Further, the peak of $\left\|S_{H_\infty}\right\|$ is minimized to ensure robustness to uncertainties compared to the peak of $\|S_{PID}\|$ at 2 Hz. T_{H_∞} also has higher -3dB bandwidth at 0.47 Hz compared to 0.2 Hz obtained from T_{PID} and a fast roll-off rate at high frequencies for noise attenuation. As shown in Fig. 2(d), the simulation and the experimental data match quite well up to 10 Hz after the controller is implemented.

Fig. 3 (a) shows that $V(t)$ can track the given $V_{ref}(t)$ well (within less than 10% error). The implemented controller shows that it adequately tracks $V_{ref}(t)$, which requires a tracking bandwidth of only 0.01 Hz (<0.1 Hz). Both transient and extensional viscosity stages of the drawing process are shown in Fig. 3 (b). As seen, the transition to extensional viscosity occurs when $dF_d/dL_p < 0.65\max(dF_d/dL_p)$.

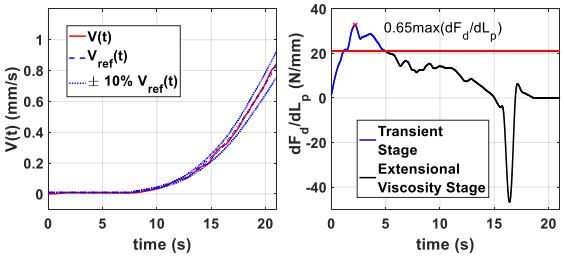

(a) (b)

Fig. 3 (a) Tracking performance; **(b)** dF_d/dL_p of the controller during the drawing process

5. Application to the BMG forming process

To demonstrate the ability of the controller, BMG blade edges samples are manufactured based on $V_{ref}\ (t)$ derived from Section 2 at T_d of 683 ± 0.03 K [10] with D_o of 20 µm. The controller could produce blades edges consistently as shown in Fig. 4. The blade quality assessment is then performed. The wedge angle is found to be $45.6° \pm 0.7°$ comparable to $45°$ mold of the testbed. The surface roughness is measured using profilometer along the length of the blade surface. R_a from 5 samples is measured to be 18 ± 8 nm, which is close to the roughness of the mold die. Blade straightness is determined as root mean squared error from the least square error fit of the blade data measured from the confocal microscope. The straightness of 5 blade samples is found to be 1.2 ± 0.8 µm and 2.1 ± 0.9 µm along the top (X-Z) view and the side (X-Y) view [4], respectively (See Fig. 5 (a) and 5 (b)). Blades manufactured from this controller are found to be straighter than the ones produced in previous studies [4]. The edge radius of the sample is measured vertically using a confocal microscope as shown in Fig. 5 (c). The blade edge radius measurement of 5 blades is found to be 55 ± 10 nm.

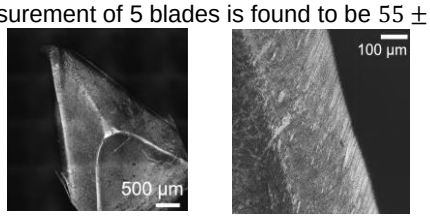

Fig. 4. Blade sample from the proposed controller

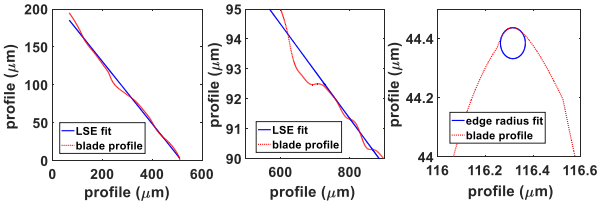

(a) (b) (c)

Fig. 5. Straightness measurement of the blade in **(a)** X-Z plane, **(b)** X-Y plane, and **(c)** edge radius measurement.

6. Conclusion

1. The design of a new reference velocity profile is proposed based on the viscoelastic stretching of a filament and thermoplastic behavior of BMG. A transitional mechanism is developed to accommodate both transient and extensional viscosity behavior of the drawing process.
2. Based on system identification of the drawing module of the testbed, H_∞ control architecture and its implementation are developed by achieving the temporal bandwidths imposed by $V_{ref}(t)$.
3. The newly developed controller can achieve better performance in terms of performance tracking and robustness to uncertainties inherent in the drawing process compared to the original PID controller.
4. BMG samples processed from this study are presented. Thermoplastic deformation of the blade edges can maintain good quality in the Newtonian region with better straightness and more consistent edge radius, respectively.

Acknowledgments

This research was carried out in part in the Frederick Seitz Materials Research Laboratory Central Facilities, University of Illinois.

References

1.Li HF, et al. "Recent advances in bulk metallic glasses for biomedical applications," Acta biomaterialia. 2016 May 1;36:1-20.

2. Lu J, et al. "Deformation behavior of the Zr41. 2Ti13. 8Cu12. 5Ni10Be22. 5 bulk metallic glass over a wide range of strain-rates and temperatures," Acta materialia. 2003 Jul 16;51(12):3429-43.

3. Krejcie AJ, et al. "A hybrid process for manufacturing surgical-grade knife blade cutting edges from bulk metallic glass," J Manuf Process. 2012 Jan 1;14(1):26-34.

4. Zhu J, et al. "Development of a Hybrid Thermoplastic Forming Process for the Manufacture of Curvilinear Surgical Blades From Bulk Metallic Glass," J Micro Nano-Manufacturing. 2017 Mar 1;5(1).

5. Dancholvichit N, et al. "An Auto-Regressive Exogenous-Based Temperature Controller for a Hybrid Thermoplastic Microforming of Surgical Blades From Bulk Metallic Glass," J Micro Nano-Manufacturing. 2020 Jun 1;8(2).

6. Anna SL, et al. On controlling the kinematics of a filament stretching rheometer using a real-time active control mechanism. J Nonnewton Fluid Mech. 1999 Nov 15;87(2-3):307-35.

7. Anna SL, et al. Elasto-capillary thinning and breakup of model elastic liquids. J Rheol. 2001 Jan;45(1):115-38.

8. Alexandrou AN, et al. "Breakup of a capillary bridge of suspensions," Fluid Dyn. 2010 Dec;45(6):952-64.

9. Dodds S, et al. "Stretching and slipping of liquid bridges near plates and cavities," Physics of Fluids. 2009 Sep 10;21(9):092103.

10. Dancholvichit N, et al. "Temperature regulation for thermoplastic micro-forming of bulk metallic glass: Robust control design using buck converter," J Manuf Process. 2020 Aug 1;56:1294-303.

11. Hsu J Da, et al. "Design and implementation of a voice-coil motor servo control IC for auto-focus mobile camera applications," PESC Record - IEEE Annual Power Electronics Specialists Conference. 2007; Jun 17 p. 1357-1362.

12. Skoczowski S, et al. "A method for improving the robustness of PID control," IEEE Trans Ind Electron. 2005 Dec 5;52(6):1669-76.

13. Skogestad S, et al. Multivariable Feedback Control: Analysis and Design. New York: Wiley; 2007